

ESA Sea Level CCI+

Algorithm Development Plan and Report

Nomenclature: SLCCI+_ADP_057_AlgoDevPlan

Issue: 2.0


Date: Dec. 10, 24



**Chronology Issues:**

Issue:	Date:	Reason for change:	Author
1.0	17/01/23	Initial Version	P. Prandi (CLS)
2.0	24/06/24	Final version	P. Prandi, A Mangilli (CLS)
3.0	10/12/24	Adaptation to 2024-2026 activities	P. Prandi, A Mangilli (CLS)

People involved in this issue:

Written by:	P Prandi (CLS), A Mangilli (CLS)	
Checked by:	JF Legeais (CLS)	16/12/24 
Approved by:	JF Legeais (CLS)	

Acceptance of this deliverable document:

Accepted by ESA:	S. Connors (ESA)	<date>	<Signature>
------------------	------------------	--------	-------------

Distribution:

Company	Names	Contact Details
ESA	S. Connors M. Restano	Sarah.Connors@esa.int ; Marco.Restano@esa.int
CLS	J.-F. Legeais ; P. Prandi ; A Mangilli ;	jlegeais@groupcls.com ; pprandi@groupcls.com ; amangilli@groupcls.com ;
LEGOS	A. Cazenave ; B. Meysignac ; F. Birol; F. Nino; F. Leger; L. Leclercq; L. Tolu	anny.cazenave@gmail.com ; Benoit.Meyssignac@univ-tlse3.fr ; florence.biol@univ-tlse3.fr ; fernando.nino@ird.fr ; fabien.leger@univ-tlse3.fr ; lancelot.leclercq@univ-tlse3.fr ; lena.tolu@univ-tlse3.fr
NOC	S. Jevrejeva	Sveta@noc.ac.uk ;
DGFI-TUM	M. Passaro	marcello.passaro@tum.de



List of Contents

1. Introduction 4

2. Local sea level rise uncertainty estimate 4

 2.1. Mathematical statement 4

 2.1.1. Current formalism for the estimation of SL trend and acceleration 4

 2.1.2. Improved formalism: optimal estimation of SL trend and acceleration 5

 2.2. Implementation and results 5

 2.2.1. Two-dimensional covariance functions..... 5

 2.2.2. Optimal analysis of Sea Level data at regional scales..... 10

 2.3. Perspectives of activities for 2024-2026 13

3. Use of 2D SWOT swath to link altimetry and tide gauges measurements 13

4. Conclusions 14

5. List of references 15

List of figures

Figure 1: Example of a space/time error covariance function 6

Figure 2 : Illustration of the position of the subdomain used in this report 7

Figure 3 : Local sea level time series within the subdomain used in this report..... 8

Figure 4 : Local sea level time series within the subdomain and the result of a regional fit of a linear model (red line) 8

Figure 5 : Noise correlated space/time error covariance matrix for the subdomain used in this report..... 9

Figure 6 : Regional sea level trend uncertainty (1 sigma) as a function of the spatial error covariance scale 10

Figure 7 : Illustrative example of the SL noise covariance matrix (left) and correlation matrix (right) for a grid point in the South Pacific Ocean 10

Figure 8 : Example of MSL timeseries with the GLS fit with a linear model (orange) and a quadratic model (green) for a grid point in the South Pacific Ocean. 11

Figure 9 : Results of the estimation of the MSL trend (top row plots) and the associated uncertainties (bottom row plots)..... 11

Figure 10 : Results of the estimation of the MSL acceleration (top row) and the associated uncertainties bottom (row) 12

List of acronyms

CCI+	Second phase of the ESA Climate Change Initiative program
ESA	European Space Agency



1. Introduction

This document provides the details of the algorithm implementation, and the main results obtained related to different tasks performed within the coastal Sea Level Climate Change Initiative project.

The main activity addresses local sea level rise uncertainty estimations. This builds on activities performed in the frame of the previous phase of the project where we estimated uncertainties on local sea level trends and accelerations (Prandi et al., 2021) based on a local derivation of the error budget approach used at global scale by Ablain et al. (2019). It describes a way to generalize the previous study with, on one side, the introduction of an optimal estimator for the estimation of the Sea Level trend and acceleration that allows to get smaller parameters uncertainties with respect to current constraints, and, on the other side, the inclusion of a spatial dependency of error covariance functions and a way to invert the parameter estimation equations on any (chosen) region of interest.

The second activity addresses the use of 2D SWOT swath to link altimetry and tide gauges measurements.

2. Local sea level rise uncertainty estimate

2.1. Mathematical statement

2.1.1. Current formalism for the estimation of SL trend and acceleration

The estimation of the MSL trend and acceleration at both global and regional scales has been based so far on the extended least squares formulation (see e.g. Ablain et al. 2009, Ribes et al. 2016, Ablain et al. 2019, Prandi et al. 2021) (hereinafter “extended ordinary least square”), which consists of applying an unweighted ordinary least square estimator (OLS) with a revisited distribution to account for the error covariance matrix in the estimation of the parameters’ uncertainties (but not in the fit). Let y be the sea level observations and X be a set of coordinates indicating when (or where) these observations are made. The regression model can be written as $y = X\beta + \varepsilon$ where ε denotes deviations from the model and β are the model parameters to be estimated.

If ε follows a normal law of mean 0 and covariance Σ , then the variance of the parameter’s estimator is given by

$$\hat{\beta} = N(\beta, (X^t X)^{-1} X^t \Sigma X (X^t X)^{-1})$$

From which the uncertainty on model parameters can be deduced (at any given confidence level).

The error budget is used to build Σ by summing individual contributions from the error terms considered (orbit, wet tropospheric correction, ...).

In Ablain et al. (2019) and Prandi et al. (2021) only the time dependency of errors is considered, ie y and ε are functions of time only. This implies that the spatial scale of the analysis is driven by the time/space scale at which the error budget was derived:

- 10 days, global in Ablain et al. (2019)
- 1 year, 2° in Prandi et al. (2021)

The algorithm development described in Sec. 3.2 aims at addressing this limitation by generalizing to two-dimensional error covariance functions that can be used at any chosen regional analysis scale.



2.1.2. Improved formalism: optimal estimation of SL trend and acceleration

Although, so far, the MSL analysis, at both global and regional scales, has been performed by using the extended least squares estimator described in sec 2.1, this is not an optimal and unbiased estimator for the estimation of the MSL trend and acceleration because the MSL covariance matrix shows a non-uniform variance and a highly correlated noise with non-negligible off diagonal terms. In this case the unweighted OLS described in Sec. 2.1 is no longer optimal, meaning that the parameters' uncertainties are overestimated, nor unbiased. In order to have an optimal and unbiased estimation of the model's parameters a General Least Square (GLS) estimator must be used. The GLS estimator is defined as:

$$\hat{\beta} = \operatorname{argmin}[(\mathbf{y} - \mathbf{m})^T \Sigma^{-1} (\mathbf{y} - \mathbf{m})]$$

Where \mathbf{y} is the vector of the data (that is, the MSL observations), $\mathbf{m}=\mathbf{m}(\mathbf{X})$ is the vector of the model (linear model for the estimation of the trend and quadratic model for the estimation of the acceleration) and Σ^{-1} is the inverse of the MSL noise covariance matrix. Weighting the residual vector by the inverse of the noise covariance matrix allows to correctly account for the noise covariance in the parameters estimation and to ensure that the parameters uncertainties are estimated at the minimum variance. This formalism is general and can be applied for the MSL analysis at global (see e.g. Mangilli et al. OSTST 2023) and regional scales, and with the extended formalism of the noise covariance matrix that includes both the temporal and spatial correlations.

2.2. Implementation and results

2.2.1. Two-dimensional covariance functions

The first algorithm change is to implement two-dimensional covariance function estimations, based on existing error covariance models (bias, drift and correlated noise).

We will implement exponentially decaying covariance functions in the space dimension, time-dependent models are left untouched.

This will be implemented under the assumption that time/space covariances are negligible, meaning that $\Sigma_{i,j} = f(t_i, t_j, x_i, x_j)$ can be written as $\Sigma_{i,j} = f_t(i, j) \times f_x(i, j)$.

An example of such covariance functions is given below (for a correlated noise in both time and space):

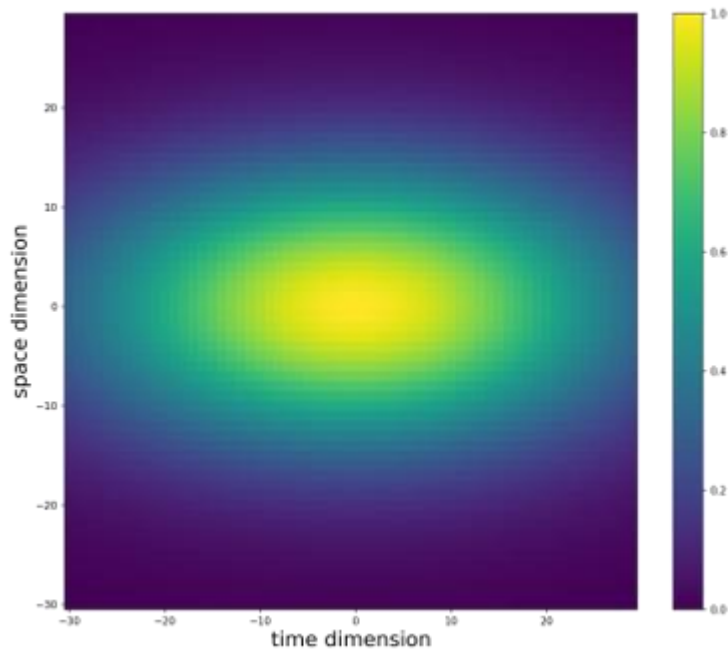


Figure 1: Example of a space/time error covariance function

Regional inversion:

The scientific goal of this algorithm is to estimate regional sea level trends and uncertainties. The algorithm therefore performs one estimation over a user-defined region of interest from all measurements that fall into this region. Here we illustrate the algorithm over a small 3 by 3 boxes domain in the Indian Ocean. The data is taken from the dataset used by Prandi et al. (2021) and is therefore available on a 2° by 2° cartesian grid.

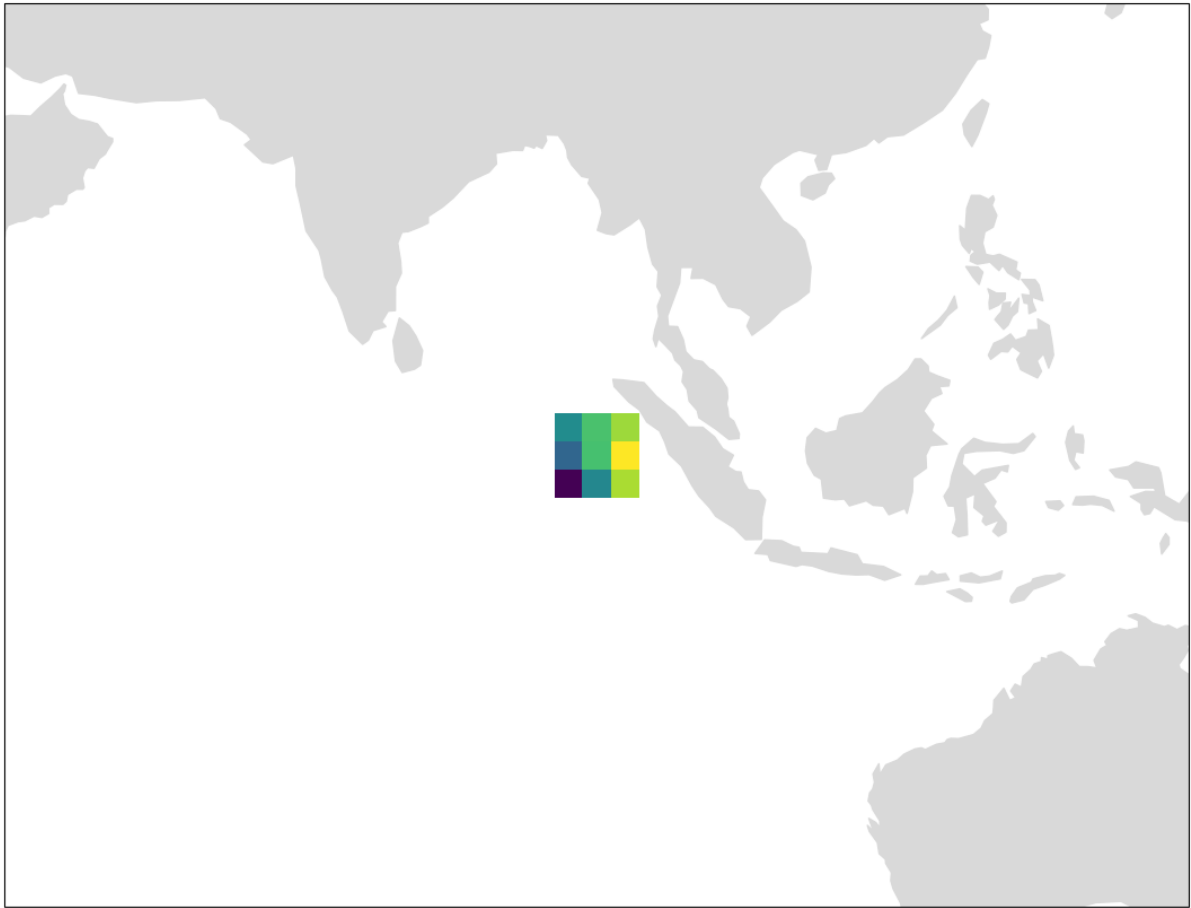


Figure 2 : Illustration of the position of the subdomain used in this report

All sea level time series that fall within this subdomain are plotted as an illustration below,

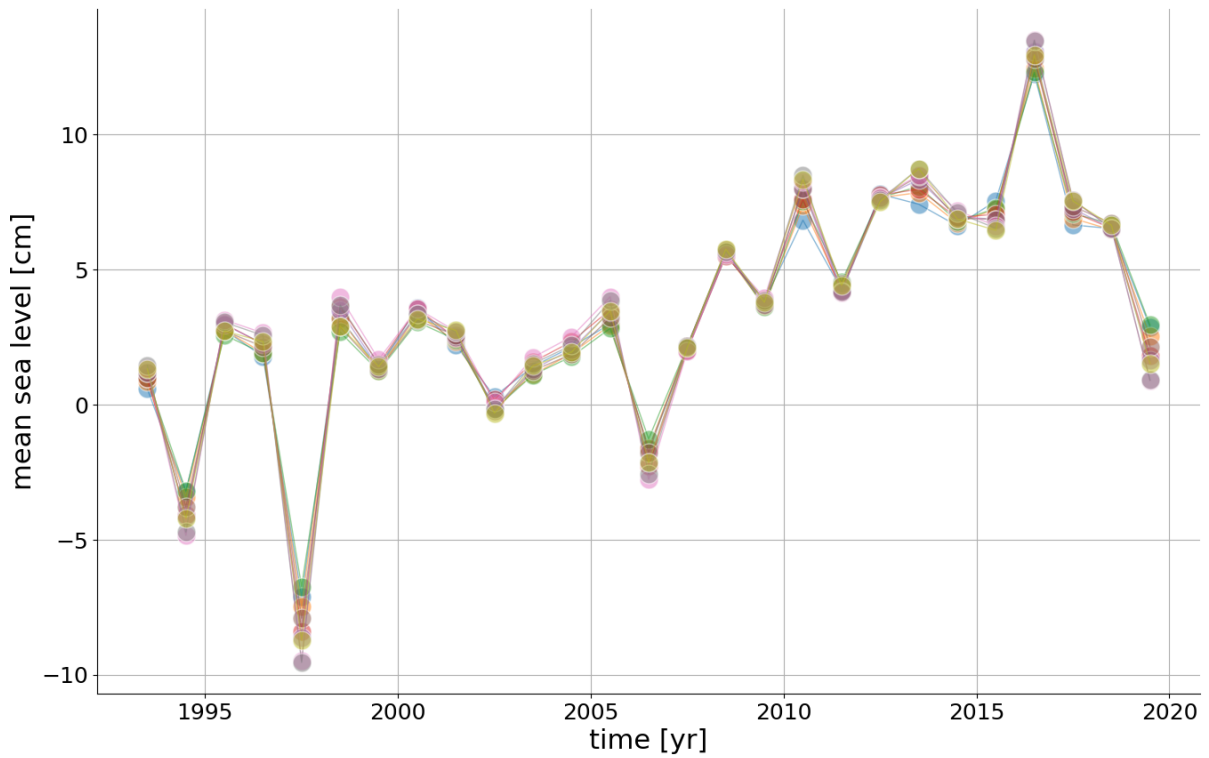


Figure 3 : Local sea level time series within the subdomain used in this report

A model (here a linear model, red line) is fitted to all available data in the subdomain and provides one regional sea level trend estimate. Model parameters are estimated following an ordinary least squares fit. Here the regional sea level trend is 3.56 mm/yr.

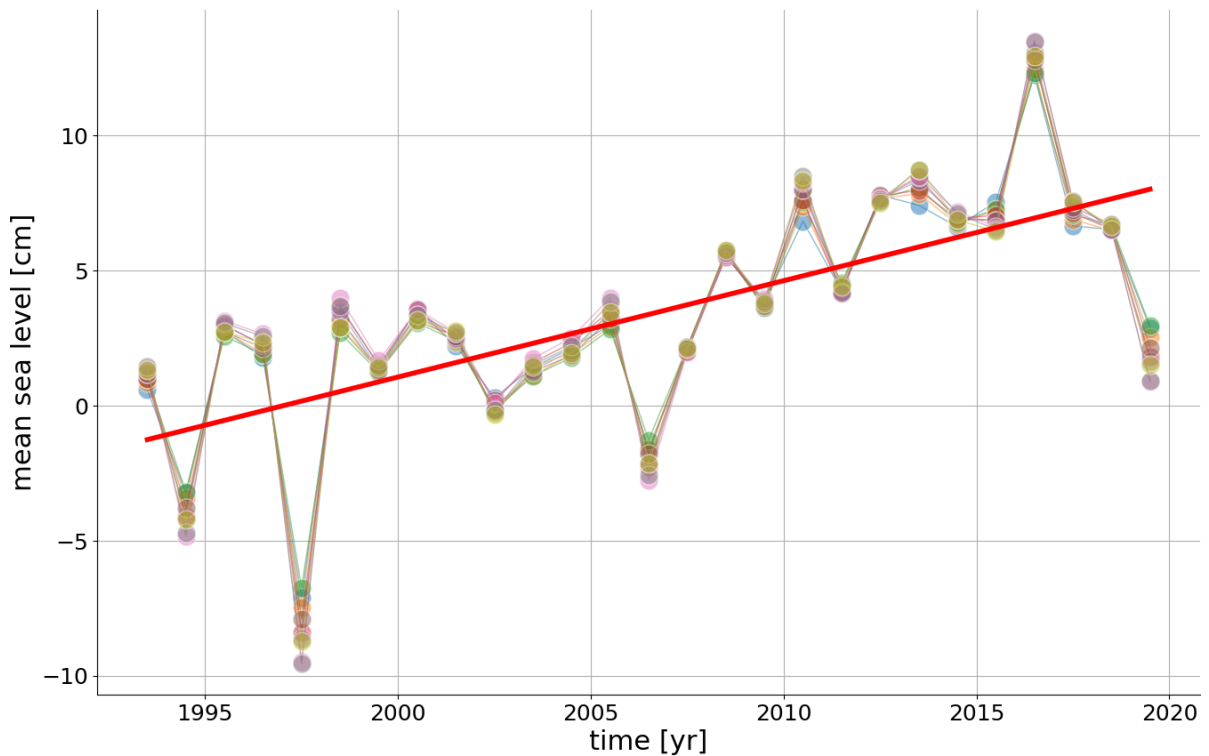


Figure 4 : Local sea level time series within the subdomain and the result of a regional fit of a linear model (red line)



The error covariance matrix is constructed blockwise after flattening the coordinates of input measurements. An example of a regional error variance/covariance matrix is given below for the same subdomain in the Indian Ocean:

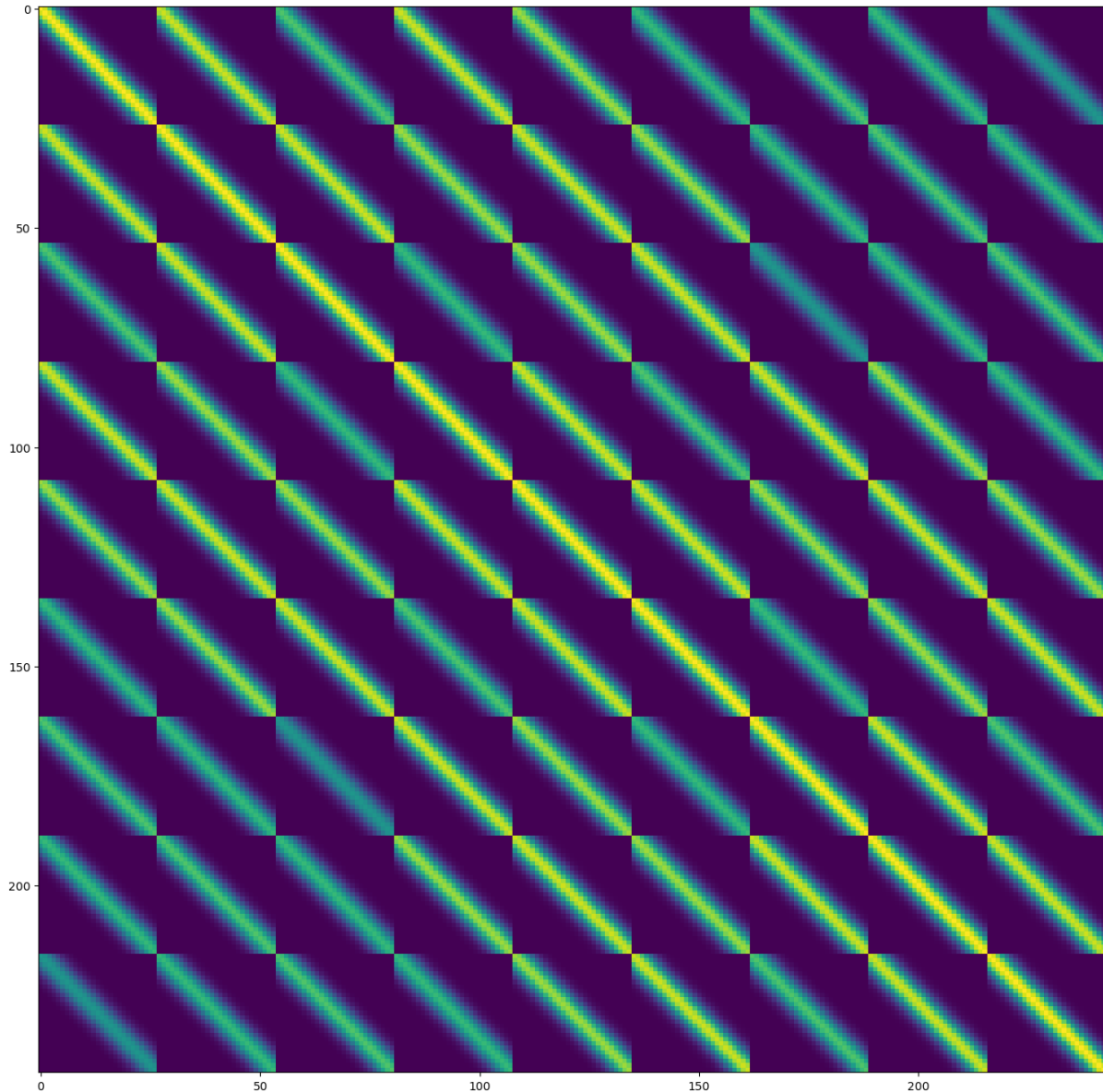


Figure 5 : Noise correlated space/time error covariance matrix for the subdomain used in this report

The matrix is constituted of 81 (9*9) sub-blocks corresponding to the 9 pixels (3*3) of the subdomain. Each block is of size 27*27 corresponding to the 27 yearly sea level estimates in the original dataset. For the sake of clarity, the error covariance model used here is a simple exponential decay in both time and space. Error decorrelation scales are set to 1000 days (roughly 3 years) and 5 degrees.

Estimating model parameter uncertainties is performed following the modified OLS formulation (not the updated Generalised Least Squares). In the simplified example that is presented here, the uncertainty on the regional trend is +/- 0.07 mm/yr at the 1 sigma level.

A simple verification is to change the error covariance scale and monitor how the uncertainty changes. Longer error covariance scales should result in higher regional uncertainties on model



parameters. For the linear model mentioned above, we increase the spatial error covariances and compute model parameter uncertainties. The result is shown below:

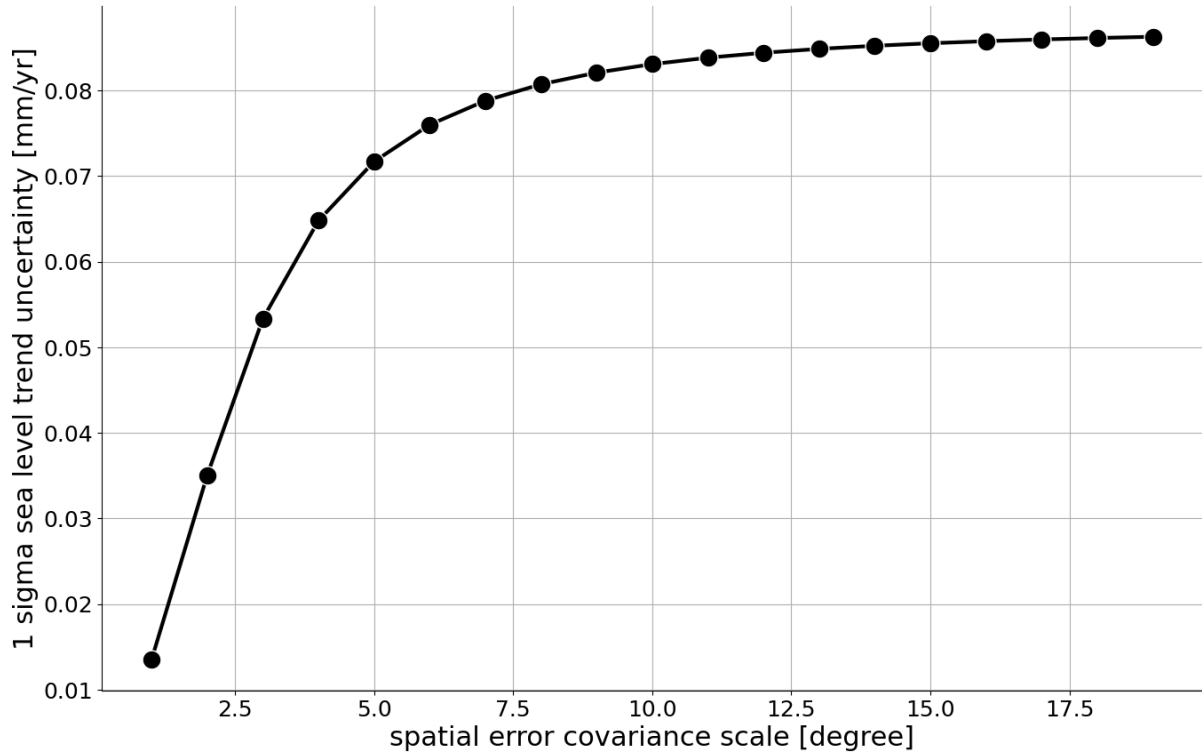


Figure 6 : Regional sea level trend uncertainty (1 sigma) as a function of the spatial error covariance scale

As expected, uncertainties increase with error covariance scales, the uncertainty reaches a plateau after about the 15 degrees covariance scale, which is 5 times the size of our domain. At this point errors are almost fully covarying over the whole domain and increasing the spatial covariance scales further does not change the error variance/covariance matrix.

2.2.2. Optimal analysis of Sea Level data at regional scales

We implemented the General Least Square analysis for the estimation of the SL trend and acceleration by using the formalism described in Sec. 2.2. As usual, the trend parameter, τ , is estimated from a linear model: $m(x)=\tau x+const$, while the acceleration, α , from a quadratic model $m(x)=bx+1/2 \alpha x^2+const$. For sake of comparison of the results with existing literature, we used the same dataset as in Prandi et al. 2021. This consist of Seal Level 2x2 degrees gridded data, yearly averaged, from 1993 to 2019. The noise covariance matrices for each grid point are the same as the ones in Prandi et al. 2021.

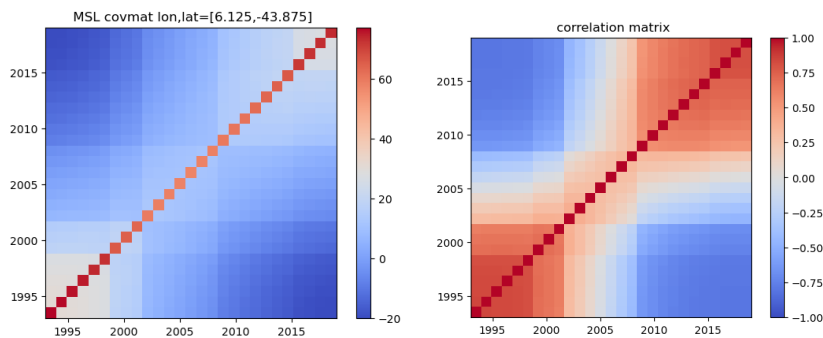


Figure 7 : Illustrative example of the SL noise covariance matrix (left) and correlation matrix (right) for a grid point in the South Pacific Ocean

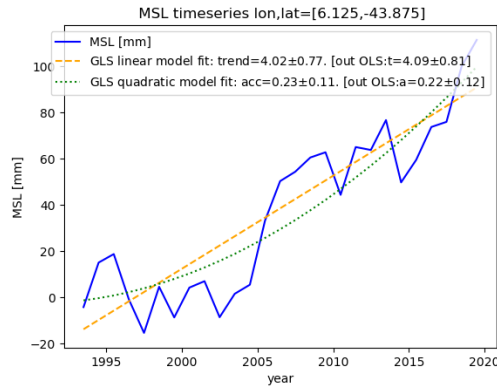


Figure 8 : Example of MSL timeseries with the GLS fit with a linear model (orange) and a quadratic model (green) for a grid point in the South Pacific Ocean.

An example of one covariance matrix for a grid point in the South Pacific Ocean (lon,lat)=[6.1,-43.8], is shown in Fig. 7.

The GLS analysis is performed on each yearly averaged MSL timeseries derived from each grid point. An example of the GLS fit of the MSL timeseries at the same grid point in the South Pacific Ocean as the covariance matrix shown above, is given in the Figure 8. The orange dashed line corresponds to the GLS fit with a linear model, while the green dotted line to the GLS fit with the quadratic model. It is worth noticing here that the acceleration uncertainties in Prandi et al. 2021 are underestimated by a factor of 2 because of a conversion error of the quadratic coefficients. We therefore corrected the values of the acceleration’s uncertainties accordingly.

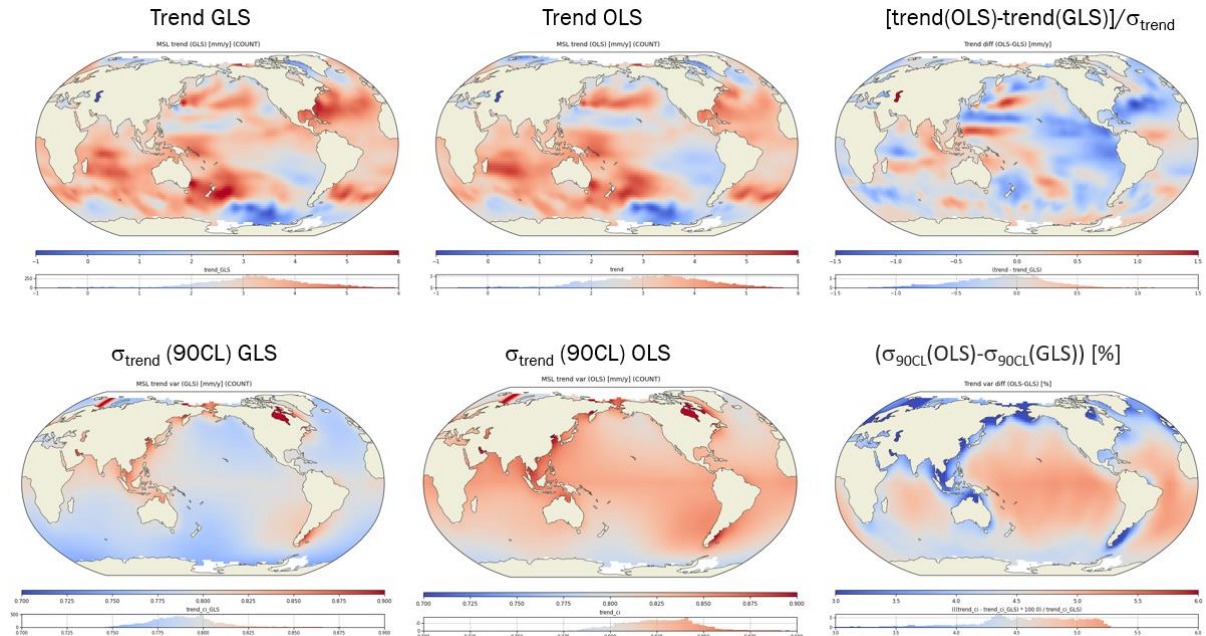


Figure 9 : Results of the estimation of the MSL trend (top row plots) and the associated uncertainties (bottom row plots)

Figure 9 and Figure 10 show the results of the GLS analysis performed on all the grid points, in comparison to the extended ordinary least square (OLS), of the estimation of the SL trend and acceleration, respectively. The two top-row plots of Figure 9 show the maps of the trend estimation as obtained with the GLS and the OLS estimator, respectively, while the third plot refers to the trend map difference between the two estimations divided by the trend uncertainty. The second-row plots show the map of the trend uncertainty from the GLS analysis (left), the extended OLS analysis (center) and the trend uncertainty map difference between the GLS and extended OLS



estimations (right). Figure 10 shares the same structure and caption as Figure 9, but displays the results for the estimation of the SL acceleration. A summary of the main findings and results is summarized below.

As expected, and as shown in the bottom-row panels of Figures 9 and 10, the parameters uncertainties, for both trend and acceleration, are always smaller in the case of the GLS because it is the optimal minimum variance estimator. Yet, the reduction of the uncertainties is less important than the reduction found at global scales when comparing the GLS-OLS analysis on the 30-year GMSL timeseries, being ~5% instead of ~15% for trend and ~20% for acceleration at global scales (see Mangilli et al OSTST 2023 for the results of the GMSL analysis). This difference could be explained by the differences in the SL variance/covariance matrix definition and construction at local scales with respect to the global scales. For instance, the temporal resolution of the GMSL timeseries is 10 days while it is of one year in the local scales analysis. The hypothesis and the terms contributing to the error budget are therefore significantly different in the two cases, making for instance the variance term dominating the error budget at local scales, while becoming subdominant with respect to the covariance terms in the GMSL case. This changes the inverse of the SL covariance matrix and thus the weights applied to the timeseries.

As shown in the top row maps of both figures, the GLS and the extended OLS analysis provide with overall compatible results of the estimation of the SL trend and acceleration, showing similar maps with similar patterns. Yet, as expected, accounting for the SL errors covariance matrix in the fit has an impact on the estimated parameters which results in differences in the trend and acceleration's values up to 1.5σ , and this impact also depends on the definition and magnitude of the variance/covariance matrix terms.

These results underline the importance of using an optimal estimator for the analysis of SL data and of constructing the most precise and realistic SL error covariance matrix as this can have a significant impact on the parameters estimation (both parameters' values and errors). The GLS estimation, being optimal and unbiased, should be used for current and future SL analysis.

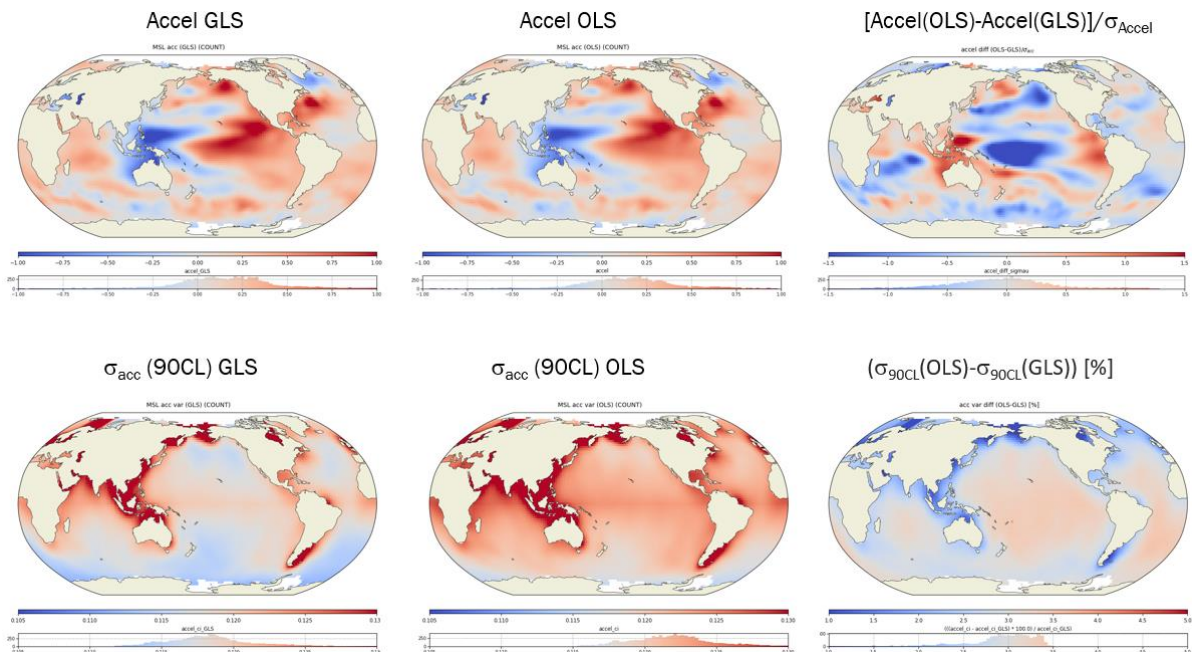


Figure 10 : Results of the estimation of the MSL acceleration (top row) and the associated uncertainties bottom (row)



2.3. Perspectives of activities for 2024-2026

During the previous phase of the SL CCI+ project, we improved our regional sea level uncertainty estimation framework (described and used in Prandi et al., 2021) with:

- the validation of an optimal estimator (Generalized Least Squares) replacing our initial Extended Least Squares formulation, resulting in a 5 to 10% reduction in MSL trend and acceleration uncertainties,
- A prototype code including a simplified (exponential decrease) model for geographical error covariances,
- A first analysis of spatial correlation scales for orbit related errors.

During the next phase of the project, the goal is to provide a framework and uncertainty budget describing time and space uncertainty covariances able to address any time/space scale of interest.

The goal of this activity is to pursue this work by:

- Porting the GLS estimator to the space/time prototype,
- Update our estimate of orbit related error correlation scales using the latest standards (POE-G),
- Estimate correlation scales for other terms of the uncertainty budget, based on scaling a simple exponential decay model as a first guess.

3. Use of 2D SWOT swath to link altimetry and tide gauges measurements

Tide gauges and altimetry both measure sea level. Tide gauges therefore provide independent reference measurements to assess altimetry. While tide gauges stations generally do not qualify as Fiducial Reference Measurements due to the lack of a SI-traceable uncertainty they still provide valuable verification information for satellite altimeter systems and are indeed used in this project to validate sea level trends at virtual stations.

Another use of tide gauges data is to detect long-term drifts in satellite radar altimeter systems (e.g., Watson et al., 2015, Valladeau et al. 2012, Mitchum et al., 2000). Comparison methods rely on a colocation method to build matchups between tide gauge height and radar altimeter measurement. These matchups are processed to build global mean estimates of the altimeter drift relative to tide gauges.

However, the spatial sampling provided by conventional nadir altimeters around tide gauges is scarce, as shown below for Sentinel-6 (red dots) around a tide gauge station at Porto Grande (Cape Verde, black dot). The snapshot below spans 2° in longitude and latitude at 16°N .

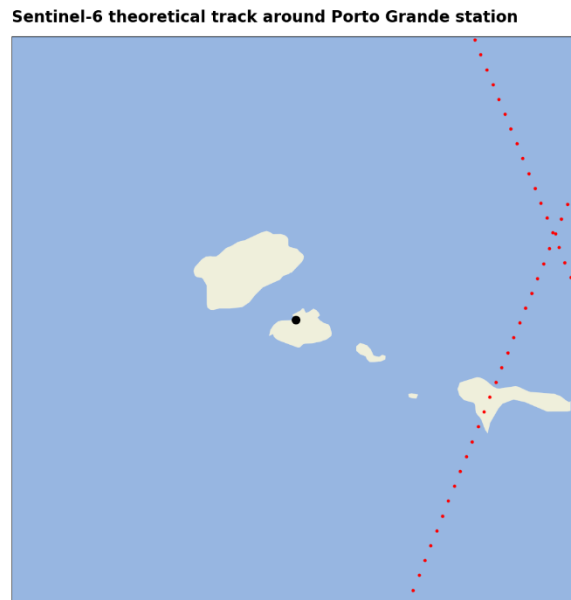


Figure 11: Sentinel-6 theoretical track around Porto Grande station

This raises the question of the accuracy of drift estimates relying on sometimes distant matchups. During the project extension we intend to analyze data from the Surface Water & Ocean Topography (SWOT) mission and compare it with our reprocessed sea level anomalies at some coastal sites. Obviously, the current lifetime of the SWOT mission (launched in 2022) is still too short to extract climate-relevant sea level trends but can provide valuable insights about spatial sea level correlation scales around either virtual or tide gauges stations. We intend to take advantage of the 2D swath of the mission to characterize the spatial scales of the SL variability and trends around virtual stations. Indeed, the sea level variability at virtual stations may rapidly change along the altimeter tracks but there is no information elsewhere (in the cross-track dimension). SWOT data will be investigated to determine if they can provide this missing information.

Results from this task will provide information on the spatial scales at which virtual stations can be reasonably considered as representative of local sea level dynamics at the coast in the cross-track dimension. It will also help to improve the method of comparison between altimetry and in situ tide gauges (commonly used to detect altimeter drifts).

4. Conclusions

A prototype code implementing a regional sea level uncertainty analysis including space/time error covariances is available at <https://github.com/pierre-prandi/2D-cov>. It implements a simple error covariance model (noise type errors only) and does provide regional sea level uncertainties. It was tested on a large domain (global between +/- 50° latitudes) on a sub sampled dataset (2° grid, yearly resolution).

Another outcome of this work is the recommendation to change the estimator used to estimate model parameters and their uncertainties. It is shown that Generalized Least Squares provide a better (less variance) model parameters estimators, thus providing lower uncertainties. In this framework the central value of model parameters estimators is also modified as it accounts for the information embedded in the error variance/covariance matrix.



5. List of references

Ablain, M., Meyssignac, B., Zawadzki, L., Jugier, R., Ribes, A., Spada, G., Benveniste, J., Cazenave, A., and Picot, N.: Uncertainty in satellite estimates of global mean sea-level changes, trend and acceleration, *Earth Syst. Sci. Data*, 11, 1189-1202, <https://doi.org/10.5194/essd-11-1189-2019>, 2019.

Mangilli, A.; Prandi, P.; Meyssignac, B.; Quet, V.; Octau, F.; Labroue, S.; Barnoud, A.; Ablain, M.; Dibarboue, G., Improvement of global mean sea level trend and acceleration uncertainties from satellite altimetry, 2023 Ocean Surface Topography Science Team Meeting, held 7-11 November, 2023. Online at <https://ostst.aviso.altimetry.fr/programs/2023-ostst-complete-program.html>, id.100. [10.24400/527896/a03-2023.3785](https://doi.org/10.24400/527896/a03-2023.3785)

Prandi, P., Meyssignac, B., Ablain, M. Spada, G., Ribes, A. & Benveniste, J., Local sea level trends, accelerations and uncertainties over 1993-2019. *Sci Data* 8, 1 (2021). <https://doi.org/10.1038/s41597-020-00786-7>

Ribes A., L. Corre, A.-L. Gibelin, B. Dubuisson, Issues in estimating observed change at the local scale - a case study: the recent warming over France. *International Journal of Climatology*, pp 3794-3806, vol 36, Issue 11, 2016. <https://doi.org/10.1002/joc.4593>



End of the document